This document is the accepted manuscript version of the following article:
Löckinger, J., Nishiwaki, S., Fuchs, P., Buecheler, S., Romanyuk, Y. E., & Tiwari, A. N. (2016). New sulphide precursors for Zn(O,S) buffer layers in Cu(In,Ga)Se2 solar cells for faster reaction kinetics. Journal of Optics, 18(8), 084002 (7 pp.). http://doi.org/10.1088/2040-8978/18/8/084002

New sulphide precursors for Zn(O,S) buffer layers in $Cu(In,Ga)Se_2$ solar cells for faster reaction kinetics

Johannes Löckinger [*,1], Shiro Nishiwaki[1], Peter Fuchs[1], Stephan Buecheler[1], Yaroslav E. Romanyuk[1] and Ayodhya N. Tiwari[1]

[1] Laboratory for Thin Films and Photovoltaics, Empa-Swiss Federal Laboratories for Materials Science and Technology, Ueberlandstr. 129, 8600 Duebendorf, Switzerland

Keywords Zn(O,S), buffer layer, CIGS, thioamide

* Corresponding author: e-mail johannes.loeckinger@empa.ch, Phone: +41 58 765 4958, Fax: +41 58 765 1122

The development of a novel chemistry for the chemical bath deposition (CBD) of Zn(O,S) buffer layers for $Cu(In,Ga)Se_2$ (CIGS) solar cells is desired for a higher growth rate, hence reduced deposition time, while reducing simultaneously the required concentration of reactants. State-of-the-art recipes are based on thiourea as sulphide precursor requiring a high molarity of reactants and relatively long deposition times due to the slow decomposition rate of thiourea. In this contribution thioamide based sulphide precursors were investigated for their decomposition and growth behaviour. A co-solvent approach in an ethanolic /aqueous ammonia medium was evaluated omitting the need for additional complexants. By replacing thiourea with the investigated thioamides, homogeneous dense layers of around 30 nm were grown with a greatly decreased deposition time of 8 minutes compared to 25 minutes for thiourea. Likewise, the concentration of the sulphide precursor was 40-fold reduced. The photovoltaic performance as characterized by external quantum efficiency (EQE) and current-voltage (IV) measurements, showed conversion efficiencies of 15% comparable to the thiourea based process.

1 Introduction Photovoltaic devices based on thin-film chalcopyrite $Cu(In,Ga)Se_2$ (CIGS) absorbers recently achieved power conversion efficiencies of 20.4% on a flexible polymer substrate [1] and 22.3% on a glass substrate [2] on the lab-scale. Highly efficient devices employing CdS as a buffer layer [1,3] suffer from a reduced photocurrent due to parasitic absorption ($E_{g,CdS} \sim 2.4$ eV). A potential to further increase the efficiency of such solar cells is plausible by substituting the commonly used CdS buffer layer with a wider band gap Zn(O,S). By varying the S/O ratio in $ZnO_{1-x}S_x$ the band gap can be tuned from 3.0 eV for x = 0.1 to 3.6 eV ($E_{g,ZnS}$) with a bow like minimum close to 2.7 eV for x = 0.58 as determined for sputter-deposited Zn(O,S) by Buffière *et al*. [4]. Several deposition methods for Zn(O,S) have been successfully applied, such as chemical bath deposition (CBD) [5-8], atomic layer deposition (ALD) [9,10], ion layer gas reaction (ILGAR) [11], ultrasonic spray pyrolysis (USP) [12] and sputtering [4,13,14]. An extensive review by Naghavi *et al.* [15] on alternative buffer layers for CIGS based solar cells summarizes the methods and their advantages focusing on the most promising buffer layer materials: Zn(O,S), In_2S_3 and $Zn_{1-x}Mg_xO$.

CBD-Zn(O,S) buffers yielded the highest power conversion efficiency of all alternative buffer layers [5]. In order to be considered for industry, however, factors concerning the bath chemistry, such as toxicity of precursors and necessary material input/usage, as well as the deposition speed, especially for a roll-to-roll deposition need to be taken into account. Due to the inherently different thermodynamics of the cadmium and the zinc sulfide in an aqueous ammonia medium great care has to be taken for the deposition parameters during CBD. Investigations on the solubility constants and complex formation constants which influence the coprecipitation of ZnS, $Zn(OH)_2$ and ZnO were performed by Lincot *et al.* [16]. In order to achieve the required film thickness in a reasonable time a substantially higher amount of precursor material is necessary for Zn(O,S) in comparison to CdS as illustrated in table 1. Efforts to reduce both deposition time as well as necessary material concentrations have been taken by Hariskos *et al.* [17] by exchanging the commonly used thiourea for thioacetamide with nitrilotriacetic acid (NTA) as

a necessary competitive complexing agent. Naghavi *et al.* [18] evaluated the enhanced reaction rate of thiourea by the addition of peroxides. In both cases, however, the thiourea based approach still yields higher power conversion efficiencies.

Here we extend the approach of Hariskos *et al.* [17] of exchanging the sulphide ("S^{2-}") precursor thiourea for a faster hydrolyzing thioamide but avoiding the use of additional complexing agents. In this contribution the use of 4-chlorothiobenzamide and 2-pyridinethioamide for the deposition of Zn(O,S) buffer layers for CIGS solar cells is introduced. An intermediate "S^{2-}" release, i.e. decomposition speed of the investigated thioamides in-between the slowly decomposing thiourea and the rather too fast (thus requiring e.g. NTA as complexant) reacting thioacetamide was expected, which will be discussed later. Due to the faster availability of the "S^{2-}" ion from the thioamides than from thiourea a less concentrated solution (smaller molarity of reactants) is necessary for the time dependent growth of Zn(O,S) (see table 1). The deposition itself is performed by CBD in an aqueous ammonia solution with ethanol as a co-solvent (to increase the solubility of 4-chlorothiobenzamide and 2-pyridinethioamide) and zinc sulfate as the zinc ion ("Zn^{2+}") source. The results are compared both to the thiourea based process as well as to CdS as a reference.

Table 1 Concentrations in [mol L^{-1}] of educts for CBD processes for best PV performance in own experiments and reported.

	CBD process	"S^{2-}" precursor	"M^{2+}" prec.	[NH_3]
Zn(O,S)	CdS[a]	0.022	0.0018	2
	thiourea[a]	0.600	0.150	4
	thiourea + "O-O" [14]	0.4	0.1	2
	thioacetamide [3]	0.030	0.16	7.5
	thioamide[a,b]	0.015	0.030	6

[a] this work

[b] 4-chlorothiobenzamide or 2-pyridinethioamide.

2 Experimental The CIGS absorber layers were grown on Mo coated soda-lime glass (SLG) substrates by coevaportation from elemental effusion cells in a multi-stage process as reported before [19,20]. The high-vacuum chamber (base pressure ~10^{-6} Pa) was equipped with an additional effusion cell for NaF. A NaF post deposition treatment (PDT) was performed as discussed in [21]. The composition of the CIGS layer as determined by X-ray fluorescence measurements is as followed: Cu/(In+Ga) = 0.79–0.83; Ga/(Ga+In) = 0.39–0.41; a thickness of d = 2.2–2.4 µm is determined by scanning electron microscopy (SEM).

The buffer layer deposition was performed by CBD in a 300 mL beaker (250 mL total volume of the solution) equipped with a magnetic stirring bar and heated in an ethylenglykol bath. CdS buffer layers were grown to a thickness of 50 ± 10 nm by immersing the sample for 24 minutes in an aqueous solution of cadmium acetate (1.8 mM), thiourea (22 mM) and ammonium hydroxide (2M [NH_3]) at 70°C. The sample was then rinsed with H_2O and dried in a counterflow of N_2.

For the thiourea-based Zn(O,S) deposition an aqueous solution of $ZnSO_4 * 7\ H_2O$ (10.78 g, 0.15 M) was preheated to 82°C. To this thiourea (11.42 g, 0.6 M) and ammonium hydroxide (4 M [NH_3]) were added. The sample was then immersed for 23-25 minutes, rinsed with NH_4OH (1.5 M [NH_3]) and H_2O and dried with N_2. The Zn(O,S) deposition based on 4-chlorothiobenzamide or 2-pyridinethioamide was performed according to the following protocol: $ZnSO_4 * 7\ H_2O$ (2.16 g, 30 mM) in 78 mL H_2O were preheated to 82°C. To this 102 mL NH_4OH (6 M [NH_3]) and either 4-chlorothiobenzamide (0.635 g, 15 mM) or 2-pyridinethioamide (0.511 g, 15 mM) in 70 mL EtOH were added. The sample was immersed into this solution immediately and removed after 8 minutes, rinsed with NH_4OH (1.5 M [NH_3]) and H_2O, respectively, and dried in a N_2 counterflow.

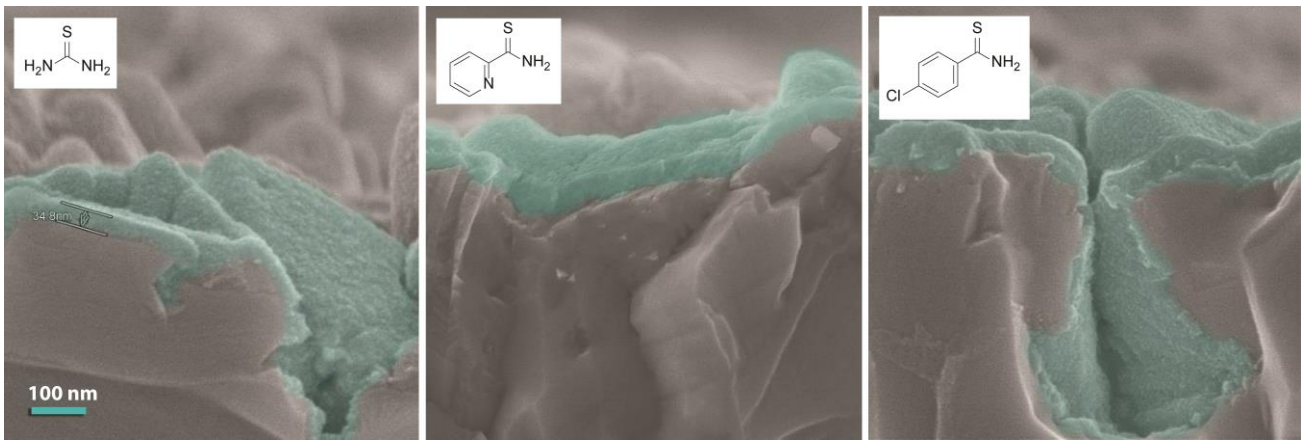

Figure 1 SEM cross-section view of surface showing the Zn(O,S) layer (colorized) on top of CIGS as used for photovoltaic devices. Scale applies to all. The layers were grown from thiourea (left), 2-pyridinethioamide (middle) and 4-chlorothiobenzamide (right).

The samples with Zn(O,S) as buffer layer were annealed at 180°C for 20 minutes directly after deposition. The resulting films are depicted in figure 1. A ~50nm thick $Zn_{0.74}Mg_{0.26}O$ layer was then sputter-deposited in an Ar-atmosphere at around 7 hPa using a power density of 0.4-1 W cm^{-2}. The cells were then finished with ~150 nm sputter deposited (2.5 W cm^{-2}, ~3 hPa) ZnO:Al (2 at%) and electron-beam evaporated Ni/Al grids. For some cells a 105 nm thick MgF_2 layer was deposited as an antireflective coating. A cell area of ~0.3 mm^2 was defined by mechanical scribing. The same procedure was applied for the CdS reference cells, except that instead of ZnMgO an intrinsic ZnO layer was deposited at 1.9 W cm^{-2} and no annealing was performed.

2.1 Analytical Methods XPS measurements were performed using a Quantum2000 from Physical Electronics with a monochromatic Al Kα source (1486.6 eV). Spectra were recorded at a base pressure below $8 \cdot 10^{-7}$ Pa. The work function of the instrument is calibrated on a regular basis to a binding energy of 83.95eV (FWHM = 0.8 eV) for the Au $4f_{5/2}$ peak. The linearity of the energy scale is checked according to ISO 15472. The spectra were recorded with an energy step size of ΔE = 0.2 eV and a pass energy of E_p = 29.35 eV. An electron flood gun operated at 2.5 eV and an ion neutralizer using Ar^+ of approx. 1 eV were used to minimize the fluctuations of the binding energy values due to sample charging. Depth profiles were obtained by Ar^+ sputtering at 1 keV for 60s per step which leads to an estimated material removal in the order of ~13 nm min^{-1}.

Solar cell performance was evaluated by *I-V* and external quantum efficiency (EQE) measurements. *I-V* characteristics were measured under simulated standard test conditions (1000 W m^{-2}, AM 1.5G, 25 °C) using a 550 W Xe Arc Lamp light source with a Keithley 2400 source meter with four-terminal sensing. EQE measurements were measured with a chopped white light source (900 W, halogen lamp) and a lock-in amplifier. A monocrystalline Si solar cell certified from Fraunhofer ISE was used as a reference cell. The cell temperature was controlled at 25 °C and a white light bias (halogen lamp, 1000 W m^{-2}) was applied.

Scanning electron microscopy (SEM) was performed on a Hitachi S-4800 electron microscope at an acceleration voltage of 5 kV.

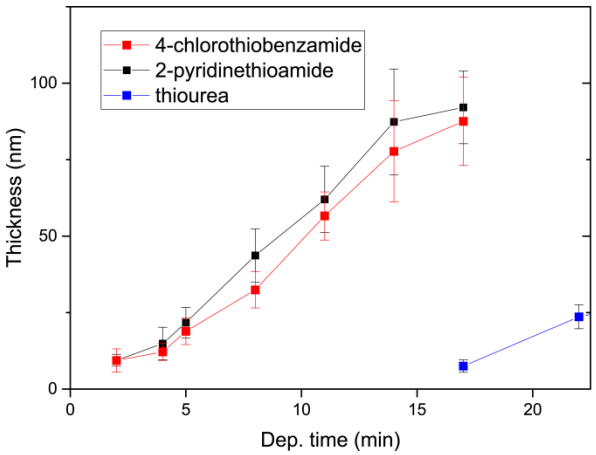

Figure 2 Growth kinetics comparing chemical bath deposition of Zn(O,S) using either thiourea, 2-pyridinethioamide or 4-chlorothiobenzamide as Sulphur sources. The substrate was SLG/Mo/CIGS and the thickness was determined by SEM. The interconnecting line is meant as a guide for the eye.

3 Results and Discussion

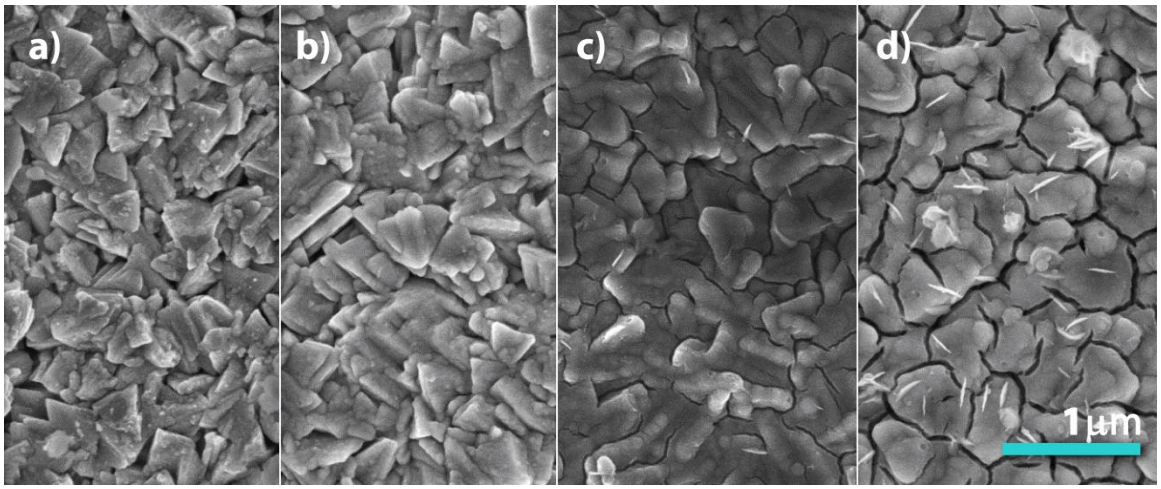

Figure 3 Topview SEM of Zn(O,S) on CIGS using 2-pyridinethioamide; deposition time a) 2 min (9 ± 2 nm), b) 5 min (22 ± 5 nm), c) 8 min (44 ± 9 nm), d) 11 min (62 ± 11 nm). In c) and d) needle/plate-shaped ZnO and ZnS crystallites which form during longer deposition times in the solution and are incorporated in the growing film are visible. Scale applies to all.

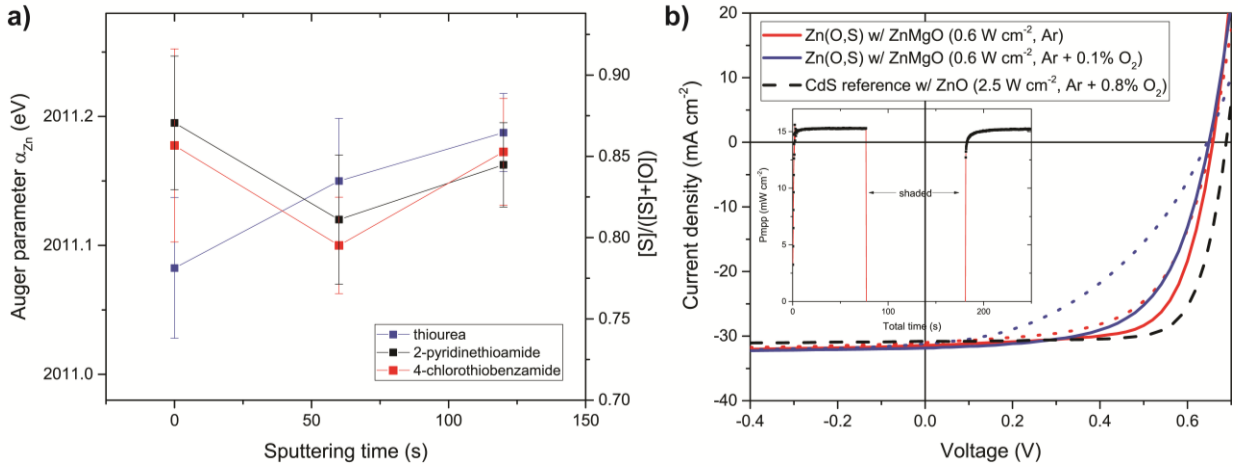

Figure 4 a) Auger parameter α_{Zn} and [S]/([S]+[O]) ratio, calculated from α_{Zn} according to Adler *et al.* [25], as a function of sputtering time for Zn(O,S) layers deposited on CIGS via the thiourea or thioamide process. The estimated sputtering rate is ~13 nm min^{-1}.
b) Current-voltage characteristics of CIGS cells employing a Zn(O,S) buffer layer deposited via TU-process comparing the influence of oxygen during the sputter-deposition of ZnMgO. The applied power to the sputtering target was set to 0.6 W cm^{-2}. The dotted line shows the as-deposited performance, the solid line shows the performance after 5 minutes of 1sun-light soaking. As a reference the CdS-buffered device is shown (dashed line). The devices comprised the same SLG/Mo/CIGS substrate and no antireflective coating was applied. The buffer layer was deposited using thiourea. The measurements were done under one sun illumination under standard testing conditions (STC)
inset: maximum power point tracking under STC of a cell employing a Zn(O,S) buffer layer deposited via the TU-based route.

3.1 Growth kinetics Shaw and Walker determined the decomposition of thiourea in aqueous solutions to be of first order with the formation of thiocyanate as the rate-determining step [22]. A proposed mechanism and the influence of electrophilicity in aromatic and heteroaromatic thioureas on the decomposition rate are discussed by Párkányi and Al-Salamah [23]. The availability of "S^{2-}" in solution at a given moment of deposition is therefore depending on the initial concentration as well as the intrinsic reactivity of the precursor itself. A different decomposition behavior, by varying –R in $RCSNH_2$ (R = NH_2, p-Cl-C_6H_4, C_5H_4N), was therefore expected to influence the growth of Zn(O,S). Figure 2 compares the growth kinetics of the thioamide based CBD process for the deposition of Zn(O,S) on a SLG/Mo/CIGS substrate to the thiourea process. The bath conditions for both the thioamide-based and thiourea-based deposition are comparable except for the higher NH_3 concentration and the solvent mixture of EtOH/H_2O in the case of the thioamide process (both modifications show no significant influence on the thiourea process). The samples are directly thereafter inserted in a vertical position upon which the timer is set. At the corresponding time the samples were removed, rinsed with NH_4OH (1.5M) and H_2O, dried in a N_2 counter flow and annealed at 180°C for 20 minutes in order to have comparable results as for the solar cell experiments. The thickness of the Zn(O,S) layer was determined from a multiple point analysis on different crystal faces using SEM on cross sections obtained by mechanical cleaving. For the thioamide based processes a higher Zn(O,S) deposition rate is clearly visible. After about 8 minutes a layer thickness of around 30-40 nanometers used for photovoltaic devices is achieved. Whereas for the thiourea-based process 22-25 minutes of deposition time are necessary.
To illustrate the growth top-view SEM pictures of Zn(O,S) on CIGS grown via the thioamide process using 2-pyridinethioamide are depicted in figure 3. The formation of the layer is visible from the different deposition times from 2 to 11 minutes. In figure 3d, displaying a ~70 nm thick layer, a cracking of the layer is visible after annealing at 180°C which is probably due to thermal stress and degassing of H_2O. In figure 1 a SEM cross-sectional view on the Zn(O,S) layer grown by the thiourea and thioamide processes is shown. A dense and homogeneous layer fully

Table 2 Current-voltage characteristics of best performing solar cells employing the same SLG/Mo/CIGS substrate with either CdS or Zn(O,S) as buffer layer and the according current densities derived from external quantum efficiency measurement.

	IV - parameters				EQE current density [mA cm^{-2}]	
	V_{OC} (V)	J_{SC} (mA cm^{-2})	FF (%)	η (%)	bias light	with -0.48V bias
CdS	0.692	31.3	77.9	16.9	31.3	
Zn(O,S) - thiourea recipe	0.650	32.4	72.9	15.4	29.8	32.8

covering the surface of CIGS is visible which is imperative for a good performance in a photovoltaic device. Especially in the image of the layer grown by 4-chlorothiobenzamide the exceptional coverage even in hollow features of the surface is shown, a benefit of the CBD method.

The difference in growth kinetics for the two thioamides seems to be negligible. Despite their different chemical features, i.e. a para-substituted chlorobenzene vs. an ortho-substituted pyridine, the reaction or release of "S^{2-}" in a basic medium occurs similarly. Hence the growth rate is nearly equal. The reaction mechanism was not investigated in this study. It is however noted that electronic effects of the substituent –R in $RCSNH_2$ (localized vs delocalized π-e^- density on $–NH_2$ vs $–p\text{-}Cl\text{-}C_6H_4$ and $–C_5H_4N$), mesomeric structures and stability of reaction products may influence the reaction speed.

3.2 X-ray photoelectron spectroscopy analysis was performed on Zn(O,S) layers deposited on CIGS samples by either the thiourea or thioamide based CBD process. Four samples of each process were measured. In order to evaluate the composition of the layer the modified Auger parameter α of Zn was determined. Previous studies have shown that α_{Zn}, defined as the sum of the binding energy of the Zn $2p_{3/2}$ core level and the kinetic energy of the Zn $L_3M_{4,5}M_{4,5}$ emission line, is a measure of the chemical environment of zinc [24,25]. A Shirley background correction was applied to the Zn $L_3M_{4,5}M_{4,5}$ peak followed by a deconvolution into two Gaussian-Lorentzian peaks with a fit restriction of 3.2 eV [26] for peak separation. The fine structure of the $L_3M_{4,5}M_{4,5}$ peak [27] is neglected with this fit. The higher binding energy component was then selected for the calculation of α_{Zn}. Adler *et al.* derived a linear relation of α_{Zn} as a function of the sulphide content x in $ZnO_{1-x}S_x$: α_{Zn} = 2010.10 (±0.05) eV + x·1.26 (±0.09) eV [25]. In figure 4a the Auger parameter α_{Zn} is plotted for the three Zn(O,S) deposition processes as a function of the sputtering time. On the secondary axis the estimated [S]/([S]+[O]) ratio derived from the aforementioned formula by Adler *et al.* [25] is depicted. For the thiourea based process a gradient of [S]/([S]+[O]) towards the CIGS surface seems to be present. The extent of this gradient, however, needs to be set into perspective with the measurement error and measurement artefacts. Differences in sputtering yield, i.e. selective sputtering, have not been considered in this analysis. Considering the long deposition time of Zn(O,S) in the thiourea based process due to the relatively slow decomposition of thiourea and the similar solubility constants of ZnO and ZnS [16] a higher incorporation of ZnO in the layer is promoted. The composition for the thiourea based process is well in accordance with reported values by Hariskos *et al.* [17] with a [S]/([S]+[O]) ratio of 0.77 (100 nm Zn(O,S) on a Mo/soda-lime glass substrate) as determined by sputtered neutral mass spectrometry depth profiles. Nakada *et al.* [28] report

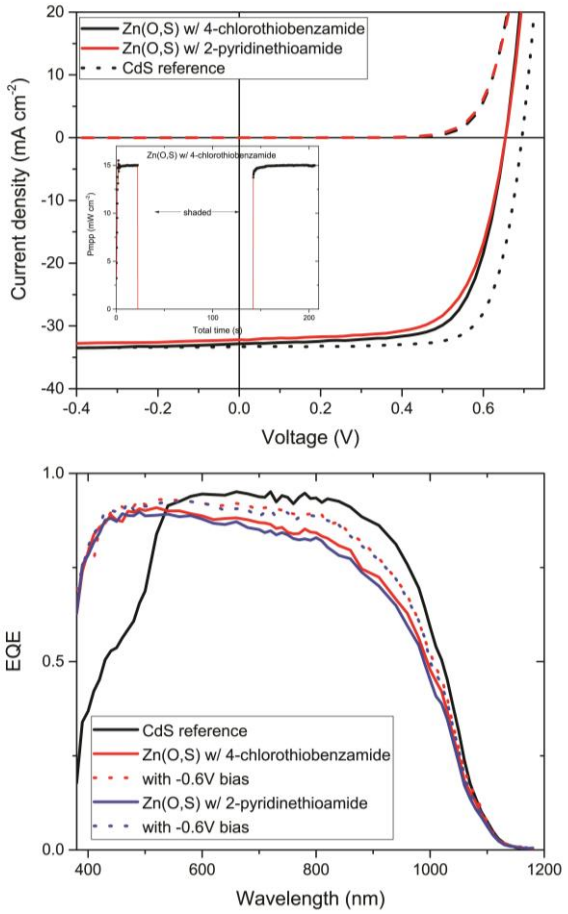

Figure 5 Current-voltage characteristics for three cells based on the same SLG/Mo/CIGS substrate and employing MgF_2 coating with the according external quantum efficiency measurement. The buffer layer was deposited using either 4-chlorothiobenzamide or 2-pyridinethioamide. The measurements were done under one sun illumination (STC). Left inset: maximum power point tracking under STC.

a graded [S]/([S]+[O]) ratio in-between 0.67 and 0.8 (120 nm Zn(O,S) on CIGS substrate) as determined by XPS depth profiles.

3.3 IV results In figure 4b, the current-voltage characteristics of photovoltaic devices employing a Zn(O,S) buffer layer deposited from commonly used thiourea are compared to cells with a CdS buffer layer. In this experiment the influence of deposition conditions for the ZnMgO window layer on the photovoltaic performance in a finished device was investigated. The influence of the oxygen concentration in the sputtering gas during the ZnMgO deposition was *i.a.* evaluated: By decreasing the oxygen content a metastable behavior in the IV-curve was mostly avoided, which is in accordance with similar studies [8]. In the case when oxygen is present simple light soaking under 1sun for 5 minutes is not sufficient to reach a decent performance. A pure argon atmosphere and a low sputter

power were therefore chosen as the deposition conditions for ZnMgO minimizing the necessity for light soaking.

The device parameters of the best performing cells based on the same CIGS absorber layer in a SLG/Mo/CIGS/buffer/Zn(Mg)O/Al:ZnO/grid(Ni,Al) configuration are given in table 2.

The effect of light soaking on the device performance of a Zn(O,S) buffered device is shown in the inset of figure 4b. Using a maximum power point tracker the current density is measured at V_{mpp} under standard testing conditions (AM1.5G, 25°C). The cell was exposed to light (1sun) prior to the measurement for a few minutes therefore the maximum efficiency is immediately achieved. Upon shading the cell completely for 100 seconds the power conversion efficiency dropped by nearly 2% absolute, but recovered to its original value within a minute under 1sun illumination. No extensive heat-light soaking or UV-light treatment is needed as reported for similar devices [6,7,29].

The photovoltaic performance of the Zn(O,S) buffer layer grown via the faster thioamide-based process is evaluated in figure 5 and table 3. For these experiments antireflective coating (MgF_2) was applied on the cells. Comparing the current-voltage characteristics of the Zn(O,S) buffered sample to the CdS-reference a similar difference (absolute delta value) is observed as compared to the TU-based Zn(O,S) buffered cells. This emphasizes that within a third of the deposition time necessary for the optimized layer thickness with the TU-process an equally well performing layer can be achieved using the thioamide precursors. The comparison to the CdS-based sample again shows the improvement of the current collection in the blue wavelength region in the external quantum efficiency due to the larger bandgap of Zn(O,S). However, the overall collection in the wavelength region of 550 – 1050 nm is inferior. By applying a voltage of -0.6 V, hence widening the space charge region, an improvement is visible. The inferior quantum efficiency of Zn(O,S) compared to CdS buffered cells is not inherent to the material itself as can be seen in literature [5,17]. There is, however, a strong dependency of the band alignment and hence collection on the [S]/[S+O] ratio as investigated by Buffière *et al.* [4] and the presence of blue photons as reported by Pudov *et al.* [30]. Further optimization should therefore lead to an improvement of the current density, surpassing the CdS reference. Regarding the metastable behaviour in the current-voltage measurement a similar effect as with the TU-based Zn(O,S) buffer layer is visible: after completely shading the device for 2 minutes, optimal performance is reached within 20 seconds of 1sun light soaking.

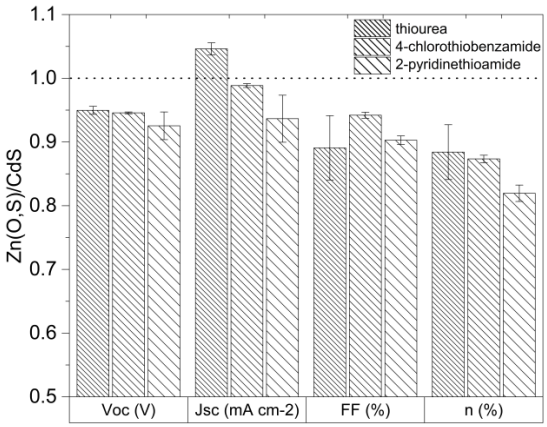

Figure 6 Comparison of IV-parameters for different Zn(O,S) processes. The data presented is the averaged cell performance (3–6 cells on a sample) of the respective experiment normalized to the corresponding CdS reference.

In order to compare the new thioamide based process with the TU process, PV parameters are averaged over the sample with the best performing cell and normalized to the respective CdS sample (see figure 6). A comparable power conversion efficiency of the process based on 4-chlorothiobenzamide to the TU process is observable, both being inferior to CdS, however. With an optimization of the [S]/[S+O] ratio in the Zn(O,S) buffer layer the PV performance can be further improved to and above the level of cells employing CdS buffer layers.

4 Conclusion This study describes a new bath chemistry and a deposition protocol for the chemical bath deposition of Zn(O,S) on CIGS. A higher growth rate, thus reduced deposition time has been achieved while simultaneously reducing the reactant concentration for both the sulphide and zinc ion precursor. Homogeneous and dense layers of Zn(O,S) were deposited on CIGS from zinc sulfate and 4-chlorothiobenzamide or 2-pyridinethioamide in an ethanolic/aqueous ammonia solution at elevated temperatures. Compared to the widely used thiourea based process the deposition time was greatly reduced from about 25 to 8 minutes for obtaining the for PV devices required film

Table 3 PV performance of the best cells in a single experiment with Zn(O,S) or CdS buffer layers on the same CIGS absorber as shown in figure 5.

	IV - parameters				EQE current density [mA cm^{-2}]	
	V_{OC} (V)	J_{SC} (mA cm^{-2})	FF (%)	η (%)	1sun	with -0.6V bias
CdS	0.695	33.3	74.7	17.3	33.2	-
Zn(O,S) - chlorothiobenzamide	0.654	32.8	69.9	15.0	32.5	34.0
Zn(O,S) - pyridinethioamide	0.654	32.2	67.3	14.2	31.8	33.7

thickness of 30-40 nm Zn(O,S). Current-voltage and external quantum efficiency measurements were performed on finished CIGS solar cells employing Zn(O,S) and CdS as buffer layers. With the new thioamide process comparable conversion efficiencies to the thiourea process have been achieved.

Acknowledgements The work was partly supported by the Swiss Federal Office of Energy (BFE) and the European Commission (FP7 project "R2R-CIGS" (project number: 283974)).

References

[1] A. Chirila *et al.*, Nat. Mater. **12**, 1107 (2013).
[2] press release 2015-12-08: Solar Frontier, http://www.solar-frontier.com/eng/news/2015/C051171.html.
[3] P. Jackson, D. Hariskos, R. Wuerz, O. Kiowski, A. Bauer, T. M. Friedlmeier, and M. Powalla, Phys. Status Solidi RRL **9**, 28 (2015).
[4] M. Buffière, S. Harel, C. Guillot-Deudon, L. Arzel, N. Barreau, and J. Kessler, Phys. Status Solidi A **212**, 282 (2015).
[5] T. M. Friedlmeier, P. Jackson, A. Bauer, D. Hariskos, O. Kiowski, R. Wuerz, and M. Powalla, IEEE J. Photovolt. **5**, 1487 (2015).
[6] T. Kobayashi, T. Kumazawa, Z. Jehl Li Kao, and T. Nakada, Sol. Energy Mater. Sol. Cells **123**, 197 (2014).
[7] T. Kobayashi, H. Yamaguchi, and T. Nakada, Prog. Photovolt: Res. Appl. **22**, 115 (2014).
[8] N. Naghavi, S. Temgoua, T. Hildebrandt, J. F. Guillemoles, and D. Lincot, Prog. Photovolt: Res. Appl. **23**, 1820 (2015).
[9] T. Kobayashi, T. Kumazawa, Z. J. L. Kao, and T. Nakada, Sol. Energy Mater. Sol. Cells **119**, 129 (2013).
[10] C. Platzer-Bjorkman, T. Torndahl, D. Abou-Ras, J. Malmstrom, J. Kessler, and L. Stolt, J. Appl. Phys. **100** (2006).
[11] R. Saez-Araoz *et al.*, Prog. Photovolt. **20**, 855 (2012).
[12] C. Fella, S. Buecheler, D. Guettler, J. Perrenoud, A. Uhl, and A. N. Tiwari, IEEE Phot. Spec. Conf., 3394 (2010).
[13] R. Klenk, P. Gerhardt, I. Lauermann, A. Steigert, F. Stober, F. Hergert, S. Zweigart, and M. C. Lux-Steiner, IEEE Phot. Spec. Conf., 853 (2013).
[14] R. Klenk, A. Steigert, T. Rissom, D. Greiner, C. A. Kaufmann, T. Unold, and M. C. Lux-Steiner, Prog. Photovolt. **22**, 161 (2014).
[15] N. Naghavi *et al.*, Prog. Photovolt: Res. Appl. **18**, 411 (2010).
[16] C. Hubert, N. Naghavi, B. Canava, A. Etcheberry, and D. Lincot, Thin Solid Films **515**, 6032 (2007).
[17] D. Hariskos *et al.*, Prog. Photovolt: Res. Appl. **20**, 534 (2012).
[18] T. Hildebrandt, N. Loones, M. Bouttemy, J. Vigneron, A. Etcheberry, D. Lincot, and N. Naghavi, IEEE J. Photovolt. **5**, 1821 (2015).
[19] J. Luo *et al.*, Adv. Energy Mater. **5**, DOI: 10.1002/aenm.201501520 (2015).
[20] A. Chirila *et al.*, Nat. Mater. **10**, 857 (2011).
[21] F. Pianezzi, P. Reinhard, A. Chirila, B. Bissig, S. Nishiwaki, S. Buecheler, and A. N. Tiwari, Phys. Chem. Chem. Phys. **16**, 8843 (2014).
[22] W. H. R. Shaw and D. G. Walker, J. Am. Chem. Soc. **78**, 5769 (1956).
[23] C. Parkanyi and M. A. Alsalamah, Z. Naturforsch. B **41**, 101 (1986).
[24] C. D. Wagner and A. Joshi, J. Electron. Spectrosc. Relat. Phenom. **47**, 283 (1988).
[25] T. Adler, M. Botros, W. Witte, D. Hariskos, R. Menner, M. Powalla, and A. Klein, Phys. Status Solidi A **211**, 1972 (2014).
[26] G. Schön, J. Electron. Spectrosc. Relat. Phenom. **2**, 75 (1973).
[27] P. Weightman, J. F. Mcgilp, and C. E. Johnson, J. Phys. C: Solid State Phys. **9**, L585 (1976).
[28] T. Nakada, T. Kobayashi, T. Kumazawa, and H. Yamaguchi, Ieee J Photovolt **3**, 461 (2013).
[29] M. Buffière, N. Barreau, L. Arzel, P. Zabierowski, and J. Kessler, Prog. Photovolt: Res. Appl. **23**, 462 (2015).
[30] A. O. Pudov, J. R. Sites, M. A. Contreras, T. Nakada, and H. W. Schock, Thin Solid Films **480-481**, 273 (2005).